# Zero-Energy State in Graphene in a High Magnetic Field

Joseph G. Checkelsky, Lu Li, and N. P. Ong
*Department of Physics, Princeton University, Princeton, New Jersey 08544, USA*
(Received 1 October 2007; published 20 May 2008)

The fate of the charge-neutral Dirac point in graphene in a high magnetic field $H$ has been investigated at low temperatures ($T \sim 0.3$ K). In samples with small gate-voltage offset $V_0$, the resistance $R_0$ at the Dirac point diverges steeply with $H$, signaling a crossover to a state with a very large $R_0$. The approach to this state is highly unusual. Despite the steep divergence in $R_0$, the profile of $R_0$ vs $T$ in fixed $H$ saturates to a $T$-independent value below 2 K, consistent with gapless charge-carrying excitations.

DOI: 10.1103/PhysRevLett.100.206801 PACS numbers: 73.63.−b, 73.21.−b, 73.43.−f

The discovery of the quantum Hall effect (QHE) in monolayer graphene crystals provides a new system for investigating relativistic Dirac-like excitations in solids [1–6]. In a magnetic field $H$, the system forms Landau Levels (indexed by $n$) that are fourfold degenerate. The Hall conductivity $\sigma_{xy}$ is accurately quantized as the chemical potential $\mu$ is changed from the hole part to electron part of the Dirac spectrum. Considerable attention has focussed on the $n = 0$ Landau Level (LL), especially on the nature of the electronic state at the charge-neutral point ($\mu = 0$) in an intense magnetic field $H$. Several groups [7–12] have predicted a high-field state with valley polarization. Experiments are actively addressing these issues [13–15]. Jiang *et al.* [14] have inferred that the sublevel gaps at $\nu = 0$ and $\pm 1$ arise from lifting of the spin and sublattice degeneracies, respectively, and inferred a many-body origin for the states. We have found that, in samples with small $V_0$ (the gate voltage needed to align $\mu$ with the Dirac point), the value $R_0$ of the resistance $R_{xx}$ at the Dirac point diverges steeply with $H$, i.e., a large $H$ drives the Dirac point to a high-resistance state. Despite the strong $H$ dependence, $R_0$ saturates to a $T$-independent value below 2 K, providing evidence for charged, gapless excitations. In samples with large $V_0$, this divergence in $R_0$ is shifted to higher fields.

Following Refs. [1,2,4], we peeled single-layer graphene crystals (3–10 $\mu$m in length) from Kish graphite on a Si-$SiO_2$ wafer. Au/Cr contacts were deposited using $e$-beam lithography [Fig. 1(a), inset]. We have found that the high-field behavior of $R_0$ is strongly correlated with $V_0$ (Table I). All samples (except K22) have $\mu$ lying in the electron band (positive $V_0$). Samples in which $|V_0| < 1$ V (K7 and K22) display a very large $R_0(14)$ (resistance measured at 14 T and 0.3 K), which arises from the strong divergence mentioned. By contrast, in samples with large $|V_0|$, $R_0(14) \leq 7$ k$\Omega$.

Figure 1(a) shows the variation of $R_{xx}$ in K7 plotted vs the shifted gate voltage $V_g' = V_g - V_0$ with $H$ held at 8, 11, and 14 T (at $T = 0.3$ K). The striking feature here is that the peak corresponding to the $n = 0$ LL increases to $>100$ k$\Omega$ at 14 T, whereas the peaks corresponding to $n = \pm 1$ remain below $\sim 7$ k$\Omega$. As in Refs. [1–5], the Hall conductivity $\sigma_{xy}$ (Panel b) displays plateaus given by [12]

$$\sigma_{xy} = \frac{\nu e^2}{h} = \frac{4e^2}{h}\left(n + \frac{1}{2}\right), \tag{1}$$

where $n$ indexes the fourfold degenerate LL and $\nu$ indexes

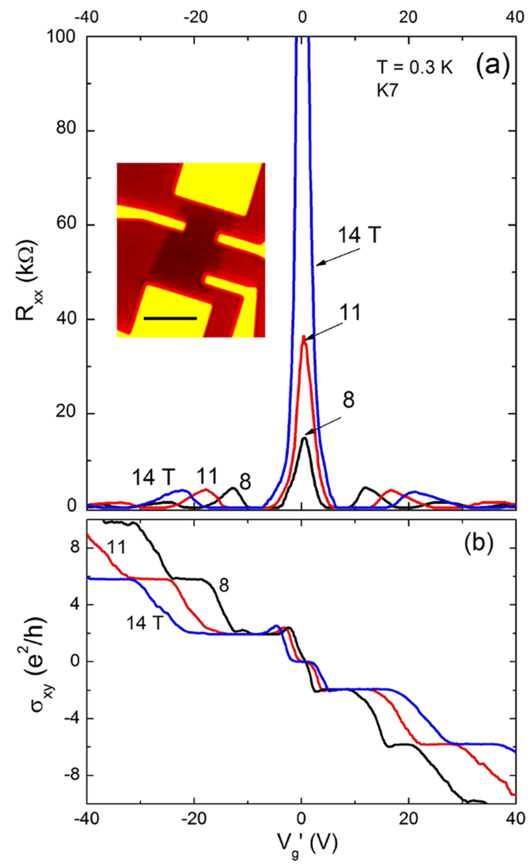


FIG. 1 (color online). The resistance $R_{xx}$ (a) and Hall conductivity $\sigma_{xy}$ (b) in Sample K7 versus (shifted) gate voltage $V_g' = V_g - V_0$ at 0.3 K with $H$ fixed at 8, 11, and 14 T. Peaks of $R_{xx}$ at finite $V_g'$ correspond to the filling of the $n = 1$ and $n = 2$ LLs. At $V_g' = 0$, the peak in $R_{xx}$ grows to 190 k$\Omega$ at 14 T. The inset shows sample K22 in false color (dark red) with Au leads deposited (yellow regions). The bar indicates 5 $\mu$m. Panel (b) shows the quantization of $\sigma_{xy}$ at the values $(4e^2/h)(n + \frac{1}{2})$. At 0.3 K, $\sigma_{xy} = 0$ in a a 2-V interval around $V_g' = 0$.

 

TABLE I. Sample parameters. $V_0$ is the gate voltage needed to bring $\mu$ to 0. $R_0(14)$ is $R_0$ measured at $H = 14$ T and $T = 0.3$ K. $\mu_e$ is the electron mobility at $H = 0$.

| Sample | $V_0$ (V) | $R_0(14)$ (k$\Omega$) | $\mu_e$ (1/T) |
|---|---|---|---|
| K5 | 3 | 80 | 0.3 |
| K7 | 1 | 190 | 1.3 |
| K8 | 12 | 15 | 0.6 |
| K18 | 20 | 7.5 | 0.9 |
| K22 | −0.6 | >280 | 2.5 |
| K29 | 22.5 | 7 | 0.2 |

individual sublevels. In K7, the "zero" plateau $\sigma_{xy} \simeq 0$ at $V_g' = 0$ is already visible at $H = 8$ T.

Narrowing our focus to the $n = 0$ LL, we examine $R_{xx}$ in the $n = 0$ LL as a function of $T$, with $H$ fixed at 14 T [Fig. 2(a)]. We see that, from 40 to 0.3 K, $R_0$ rises steeply from 4 k$\Omega$ to 190 k$\Omega$. The curve of the conductivity $\sigma_{xx}$ plotted vs $V_g'$ reveals a two-peak structure that implies splitting of the fourfold degeneracy by a gap $\Delta$ [Fig. 2(b)]. At 100 K, the two peaks are already resolved. With decreasing $T$, the minimum at $V_g' = 0$ initially deepens rapidly, but saturates below ~2 K. The Hall conductivity $\sigma_{xy}$ at 0.3 K (thin curve) displays a well-defined plateau on which $\sigma_{xy} \simeq 0$. Because the next plateau is at $\sigma_{xy} = 2(e^2/h)$, we infer that each of the peaks in $\sigma_{xx}$ is comprised of 2 unresolved sublevels. The opening of the gap causes $\sigma_{xx}$ (at $V_g' = 0$) to fall rapidly with decreasing $T$, until saturation occurs below 2 K.

The behavior of $R_0$ described here is qualitatively different from earlier reports, for, e.g., Ref. [13]. From studies on several samples (Table I), we find that the offset gate $V_0$ is a crucial parameter. Figure 2(c) compares the curves of $R_{xx}$ ($n = 0$ LL) in the samples K5, K7, K8, and K29, all measured at 14 T at $T = 0.3$ K. For each sample, we have plotted $R_{xx}$ vs the unshifted gate voltage $V_g$, so its peak automatically locates $V_0$. It is clear that K7 ($V_0 = 1$ V) has the highest peak, followed by K5 ($V_0 = 3$ V), whereas K8 ($V_0 = 12$ V) and K29 (22.5 V) have peaks that are severely suppressed. This pattern is clarified below (when we discuss $R_0$ vs $H$).

Sample self-heating may also obscure the divergence. We find that, below 1 K, self-heating becomes serious when the dissipation exceeds ~2 pW. The measurements of $R_{xx}$ vs $V_g$ were repeated at 3 currents ($I = 0.6$, 2 and 15 nA) at $T = 0.3$ K. The results at $I = 0.6$ and 2 nA are virtually identical. However, the curve at 15 nA is 30% smaller near $V_g' = 0$, consistent with heating. Hence, we have kept $I$ at 2 nA to eliminate self-heating as a problem. Heating at the contacts is negligible because of the small contact resistances (~1 k$\Omega$) relative to $R_0$.

Hereafter, we focus on $R_0$, or equivalently, the Dirac-point conductivity $\sigma_{xx}^0 \equiv L/wR_0$ ($L$ and $w$ are the length and width). Curves of the conductivity versus $\log_{10}T$ are shown in Fig. 3(a) at selected fields. In low fields ($H <$

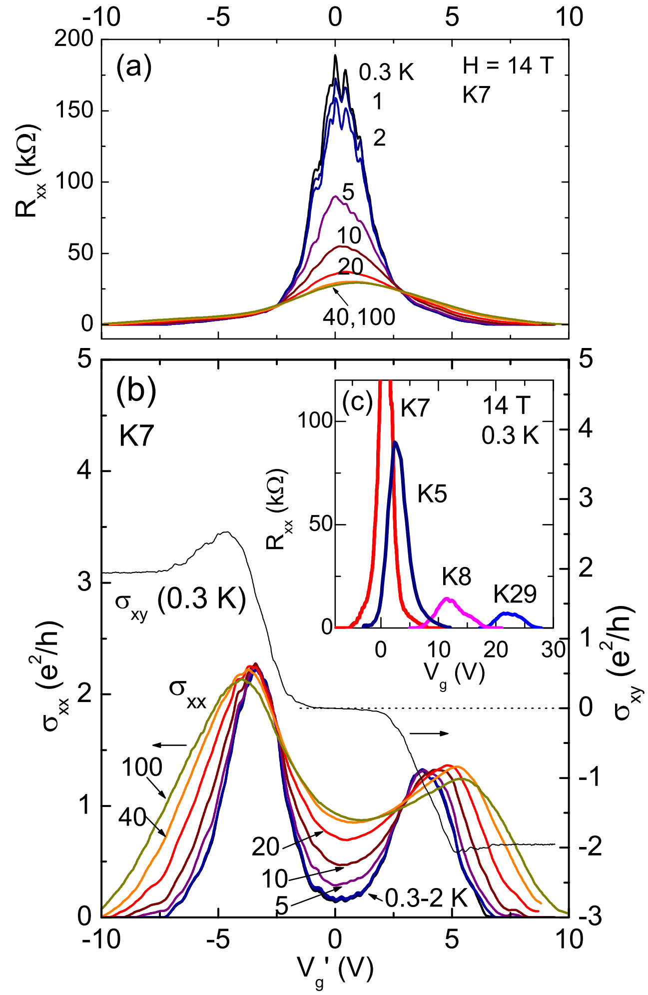


FIG. 2 (color online). The resistance $R_{xx}$, conductivity $\sigma_{xx}$ and the Hall conductivity $\sigma_{xy}$ in K7 vs the shifted gate voltage $V_g'$, with $H$ fixed at 14 T (we used [5] $\sigma_{xy} = -R_{xy}/[(wR_{xx}/L)^2 + R_{xy}^2]$). As $T$ decreases to 0.3 K, the zero-energy peak in $R_{xx}$ (Panel a) rises steeply to 190 k$\Omega$. Panel (b) shows that, as $T$ decreases, double peaks in $\sigma_{xx}$ are clearly resolved. Between the peaks, $\sigma_{xx}$ falls rapidly but saturates below 2 K. The Hall conductivity at 0.3 K (thin curve) displays a clear plateau ($|\sigma_{xy}| < 0.02e^2/h$) in the interval $-1V < V_g' < 1V$. Panel (c) compares $R_{xx}$ (of $n = 0$ LL) vs unshifted gate $V_g$ in the samples K5, K7, K8, and K29 at 0.3 K. In each sample, $R_{xx}$ peaks at $V_0$. As $V_0$ increases, $R_0(14)$ rapidly decreases.

9 T), the $T$ dependence of $\sigma_{xx}^0$ is quite mild. As $H$ is increased to 14 T, the opening of the gap $\Delta$ (between the $n = 0$ sublevels) causes the conductance to decrease sharply below 40 K. However, instead of falling to 0, $\sigma_{xx}^0$ saturates below 2 K to a $T$-independent residual value $\sigma_{\rm res}$, as anticipated in the discussion of Fig. 2(b). The existence of this residual $\sigma_{\rm res}$, which is highly sensitive to $H$, is one of our key findings.

The field dependence of $\sigma_{\rm res}$ is best viewed as a divergent $R_0$. Figure 3(b) shows the rising profile of $R_0$ vs $H$ in sample K7 at selected temperatures. The divergent form at the lowest $T$ (0.3 K) strongly suggests that the system is

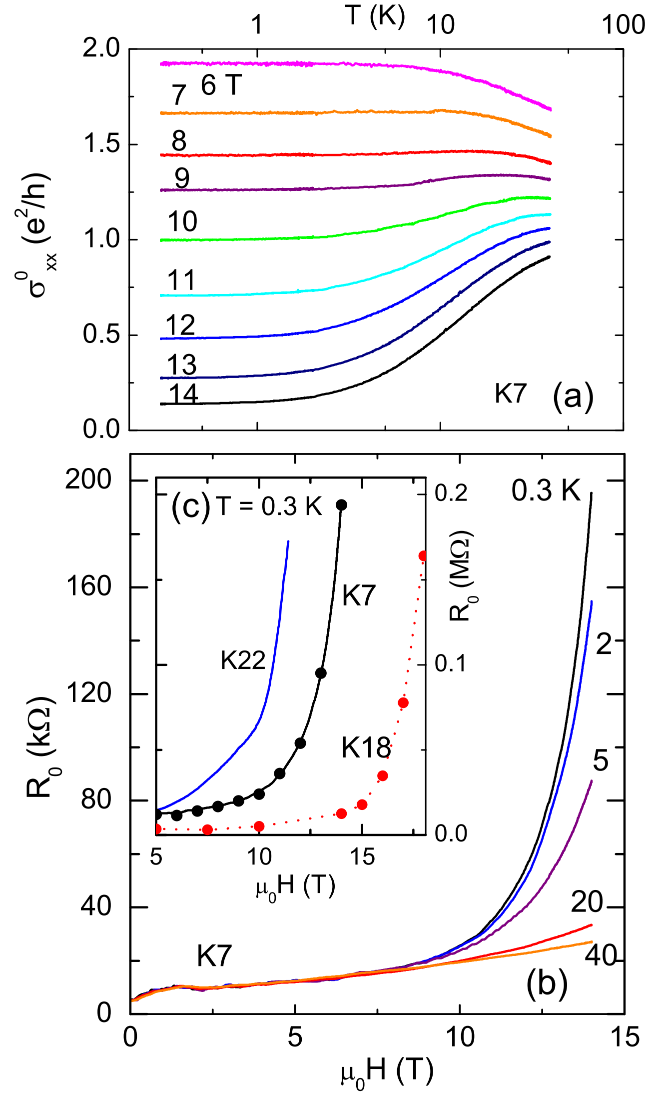


FIG. 3 (color online). The $T$ dependence of $\sigma^0_{xx}$ in K7 ($= L/wR_0$) and the $H$ dependence of $R_0$ at low temperature. Panel a shows curves of $\sigma^0_{xx}$ vs $\log_{10}T$ with $H$ fixed at 6–14 T. For $H > 8$ T, the gap $\Delta$ causes $\sigma^0_{xx}$ to decrease markedly until saturation at the residual value $\sigma_{\rm res}$ occurs below 2 K. Panel (b) displays the steep increase in $R_0$ vs $H$ in K7 at selected $T$. At 0.3 K, $R_0$ appears to diverge at a field near 18 T [see Fig. 4(b)]. Panel (c) compares the $R_0(H)$ profiles in Samples K7, K18, and K22. In sample K18 ($V_0 = 20$ V), the divergence in $R_0$ becomes apparent only above 14 T, whereas in K22 ($V_0 = -0.6$ V) $R_0$ starts to diverge at fields lower than in K7. In K7, we have plotted $R_0$ values measured by sweeping $V_g$ at fixed $H$ (solid symbols) with $R_0$ measured by sweeping $H$ with $V_g'$ fixed at 0 (solid curve), to show consistency.

rapidly approaching a field-induced crossover (or transition) to a state with very large $R_0$.

In light of the importance of $V_0$, it is instructive to see how the profile of $R_0$ vs $H$ varies between samples. Figure 3(c) compares the results in K7, K18 and K22 at $T = 0.3$ K. In K18, where $V_0$ (20 V) is quite large, the divergence in $R_0(H)$ becomes noticeable only in fields above 14 T. Conversely, in K22 for which $V_0$ ($-0.6$ V) is slightly smaller than in K7, $R_0$ diverges at field scales smaller than in K7. (Above $H = 12$ T, the curve of $R_0$ in K22 rises to very large values, reaching 9 MΩ at 33 T. However, for $R_0 > 0.5$ MΩ, it is plagued by breaks in slope and oscillations, suggestive of severe self-heating).

From the trend, it is clear that the divergence in $R_0$ is shifted to ever higher fields as $V_0$ increases. Referring back to Fig. 2(c), we now see that the strong suppression of $R_0(14)$ in samples with large $V_0$ simply reflects the shift of the divergence to larger $H$. These results underscore the importance of choosing samples with $|V_0| < 1$ V for investigating the intrinsic properties of the Dirac-point. In K7, we also checked that $R_0$ measured by varying $V_g$ at fixed $H$ or by varying $H$ in fixed $V_g$ agree numerically.

The variation of $R_0(T, H)$ in K7 is conveniently represented in a contour plot in the $T$-$H$ plane (Fig. 4). Below $\sim$2 K, the contour lines are horizontal, which implies that $R_0$ is unchanged if the sample is cooled in fixed $H$. This provides evidence that $\sigma_{\rm res}$ involves gapless excitations. However, if $T$ is fixed, $R_0$ rises steeply with $H$, implying proximity to the large-$R_0$ state (deep-red region). When a system approaches the large-resistance state, its resistivity generally diverges as $T \to 0$, as a result of either strong localization (variable-range hopping) or the opening of a mobility gap (weak localization is not relevant here because of the intense $H$). In both cases, decreasing $T$ reduces the conductance because the itinerant states are severely depopulated. Hence, the pattern in Fig. 4(a) is most unusual. The gaplessness of $\sigma_{\rm res}$ suggests that, below 2 K, these excitations are protected from the effects of changing $T$. Paradoxically, they are not protected from an increasing $H$, which reduces the current carried at an exponential rate.

One way to distinguish theories is by how the fourfold degeneracy in the $n = 0$ LL is lifted. In the theory in Refs. [13,16], the exchange energy lifts the spin degeneracy (but nominally not the valley degeneracy) in the bulk. At the edge, lifting of the valley degeneracy creates a pair of counter-propagating edge states. In the sample shown in Ref. [13], the slight increase in $R_0$ (threefold at 33 T) was explained by increased scattering between the edge states. However, in our data, this mild change with $H$ is actually seen only in samples with $V_0 > 30$ V. Samples with very small $|V_0|$ [K22 and K7 in Fig. 3(c)] are in a radically different category. In large $H$, the divergence in $R_0$ (which reaches 9 MΩ at 33 T in K22) is far too large to be explained by counter-propagating edge states. Instead, our results imply a high-field ordered state consistent with the quantum Hall insulator [7–10].

The scenario is suggested by the form of $R_0(H)$, which fits very well to the form $R_0 \sim \xi(h)^2$, where the correlation length $\xi$ has the Kosterlitz-Thouless (KT) dependence

$$\xi_{\rm KT} \sim \exp(b/\sqrt{1-h}), \qquad (h = H/H_0), \qquad (2)$$

with $H$ replacing $T$. Plotting $\ln R_0$ vs $\sqrt{1-h}$, we find that the high-field portion becomes linear [Fig. 4(b)] when $H_0$

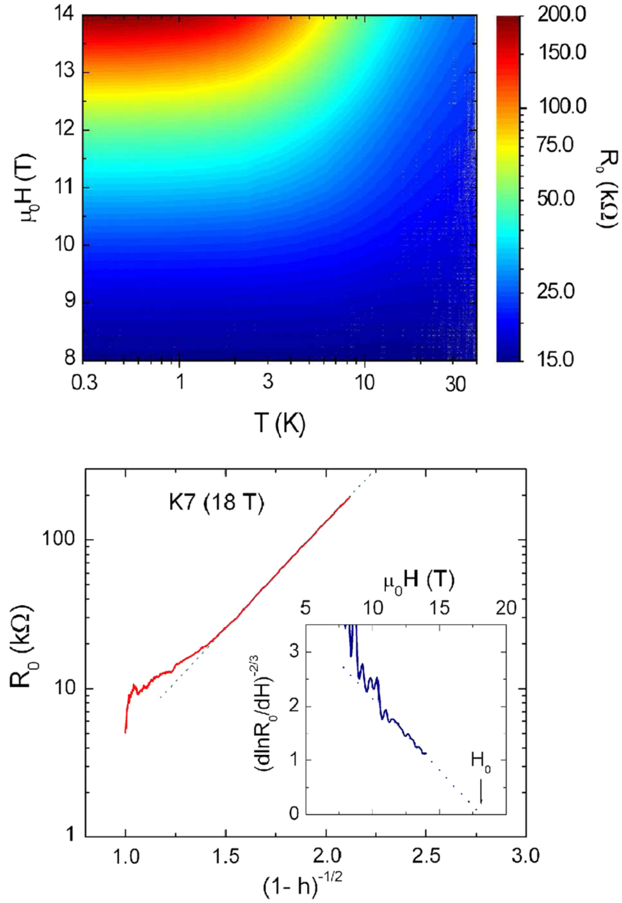


FIG. 4 (color online). (a) The contour plot of $R_0(T, H)$ (K7) in the $T$-$H$ plane (vertical bar shows values of $R_0$). The contour lines emphasize the unusual approach to the large-$R_0$ state. At low $T$, $R_0$ is unchanged on a horizontal path ($H$ held fixed), but it rises rapidly on a vertical path (increasing $H$ at fixed $T$). Panel (b) displays $\log R_0$ vs $1/\sqrt{1-h}$ in K7 at $T = 0.3$ K, with $h = H/H_0$, where $H_0 = 18$ T. The linear segment at large $R_0$ shows that the divergence is consistent with $R_0(h) \sim \exp[2b/\sqrt{1-h}]$ with $b \sim 0.7$. In Panel (c), the plot of $(d\ln R_0/dH)^{-2/3}$ vs $H$ shows a high-field linear segment that extrapolates to zero at $\sim H_0$ (18 T).

is adjusted to be 17–18 T. From the slope, we find that the parameter $b$ is $\sim$0.7, consistent with standard KT theory. For self consistency, we may also let the data determine $H_0$. By Eq. (2), we have $d\ln R_0/dH \sim (H_0 - H)^{-3/2}$. Hence a plot of $(d\ln R_0/dH)^{-2/3}$ vs $H$ should cross the $H$ axis at $H_0$. Indeed, this quantity, plotted in Fig. 4(c), becomes linear at large $H$ and extrapolates to zero at $18 \pm 0.5$ T, in agreement with Fig. 4(b).

We adopt as a working hypothesis that this reflects the approach to a KT transition. The ordered state at large $H$ is destroyed by the spontaneous appearance of defects which increase exponentially in density at $H_0$. The steep fall of $R_0$ below $H_0$ may reflect the current carried by these defects.

In the quantum Hall insulator [7–10], the exchange energy in large $H$ lifts the valley degeneracy in the $n = 0$ LL to produce a valley polarized state with a bulk gap (counterpropagating edge states are absent). The reduction of the $SU(4)$ symmetry to lower symmetries by the effects of Zeeman energy, disorder or lattice discretization is discussed in Refs. [8,10,12]. If the ordered state indeed has $U(1)$ symmetry, the $XY$ order is susceptible to a KT transition [7]. It would be very interesting to relate the fit of $R_0$ to Eq. (2) with charged, topological excitations envisioned in the KT transition. Experiments to overcome the self-heating problem at larger $R_0$ are underway to provide further evidence for a transition to the large-resistance state and to clarify its nature.

We acknowledge valuable discussions with Kun Yang, P. A. Lee, M. Lee, A. Geim, and A. Pasupathy. We are indebted to Philip Kim for generously providing Kish graphite crystals. This research is supported by NSF-MRSEC under Grant No. DMR 0213706, and by the Princeton Center for Complex Materials. Some data were taken in the National High Magnetic Field Lab., Tallahassee, which is supported by NSF and the State of Florida.

*Note added in proof.*—A field-induced transition to a CDW gapped state has been proposed by Khveshchenko [17].


[1] K. S. Novoselov *et al.*, Science **306**, 666 (2004).
[2] K. S. Novoselov *et al.*, Proc. Natl. Acad. Sci. U.S.A. **102**, 10 451 (2005).
[3] K. S. Novoselov *et al.*, Nature (London) **438**, 197 (2005).
[4] Y. Zhang, J. Tan, H. L. Stormer, and P. Kim, Nature (London) **438**, 201 (2005).
[5] Y. Zhang *et al.*, Phys. Rev. Lett. **96**, 136806 (2006).
[6] Y.-W. Tan *et al.*, Phys. Rev. Lett. **99**, 246803 (2007).
[7] K. Nomura and A. H. MacDonald, Phys. Rev. Lett. **96**, 256602 (2006).
[8] J. Alicea and M. P. A. Fisher, Phys. Rev. B **74**, 075422 (2006).
[9] Kun Yang, S. Das Sarma, and A. H. MacDonald, Phys. Rev. B **74**, 075423 (2006).
[10] M. O. Goerbig, R. Moessner, and B. Douçot, Phys. Rev. B **74**, 161407(R) (2006).
[11] D. A. Abanin, P. A. Lee, and L. S. Levitov, Phys. Rev. Lett. **98**, 156801 (2007).
[12] For a review, see Kun Yang, Solid State Commun. **143**, 27 (2007).
[13] D. A. Abanin *et al.*, Phys. Rev. Lett. **98**, 196806 (2007).
[14] Z. Jiang, Y. Zhang, H. L. Stormer and P. Kim, Phys. Rev. Lett. **99**, 106802 (2007).
[15] Sungjae Cho and Michael S. Fuhrer, Phys. Rev. B **77**, 081402(R) (2008).
[16] D. A. Abanin, P. A. Lee, and L. S. Levitov, Phys. Rev. Lett. **96**, 176803 (2006).
[17] D. V. Khveshchenko, Phys. Rev. Lett. **87**, 206401 (2001).